Photochemical & Photobiological Sciences

Cite this: *Photochem. Photobiol. Sci.*, 2012, **11**, 1929

www.rsc.org/pps

PAPER

Solid-state photochemistry of crystalline pyrazolines: reliable generation and reactivity control of 1,3-biradicals and their potential for the green chemistry synthesis of substituted cyclopropanes

Saori Shiraki, Cortnie S. Vogelsberg and Miguel A. Garcia-Garibay*

Received 24th July 2012, Accepted 16th August 2012
DOI: 10.1039/c2pp25263e

To expand on the limited number of examples that exist in the literature for the solid-state photodenitrogenation of azoalkanes, a series of crystalline 7-alkyl-2,3,7-triazabicyclo[3.3.0]oct-2-ene-6,8-diones with varying 4,4-substituents were prepared. Their photochemical behavior in solution and in the solid state was dependent on the 4,4-substitution of the 1-pyrazoline ring, with unsubstituted pyrazoline **12** giving a mixture of products both in solution and in the solid state. Diphenyl substituted pyrazolines **13** denitrogenate spontaneously in solution but require light exposure to react quantitatively in the solid state. *t*-Butyl-phenyl substituted pyrazolines **14** were shown to denitrogenate both chemo- and diastereoselectively in solution and in the solid state to yield a single product in quantitative yield.

Introduction

The environmental impact of chemical reactions as they are normally executed is a growing concern. It has been estimated that of the non-aqueous material used in pharmaceutical production, organic solvents account for 80–90% of mass used.[1] While some of the solvent may be recovered and reused, it still constitutes a large portion of cost that is generated and results in the production of waste. With growing demands for more environmentally conscious reactions, those that occur in the solid state and require no solvents constitute a promising avenue for waste reduction.[2] In this context, we have suggested that photochemical reactions in crystalline solids can be engineered in a reliable manner by considering the mechanistic information that determines the decay of excited states.[3–6] We have analyzed the formation of carbenes in crystalline diazo compounds[4] and diazirines,[5] and the formation of biradicals and radical pairs in crystalline ketones.[6] We have shown that these reactions tend to occur with very high selectivities and in high chemical yields,[7] and some solid state reactions have been used in the synthesis of natural products.[8] With the purpose of expanding the scope of solid-state photochemical reactions in green synthesis, we report here an exploratory investigation on the denitrogenation of pyrazolines.[9] The purpose of this work is to determine whether or not a set of homologous pyrazolines will react in the solid state, and whether the reaction will occur in a selective manner. The long term vision of this work, as illustrated in Scheme 1, is to look for a promising strategy for the stereospecific synthesis of chiral cyclopropanes.

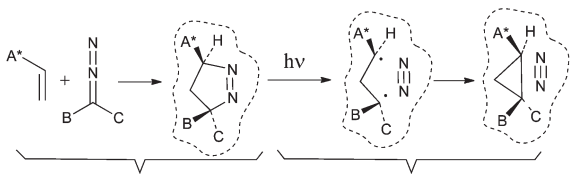

Scheme 1

The photochemistry of pyrazolines was first reported in 1960, when they were shown to provide a variety of denitrogenated products.[10] While a wide range of azoalkanes has been studied in solution since that time, only a small number of examples have been reported in the solid state.[11] The first of these studies explored the photoreactivity of *exo*- and *endo*-5-methoxy-2,3-diazabicyclo[2.2.1]hept-2-ene **1** (Scheme 2).[11a] In this case, solution photolysis of *exo*- and *endo*-**1** gave a mixture of *cis*- and *trans*-2-methoxybicyclo[2.1.0]pentane **2** with a small amount of biradical disproportionation product (5%). The solid state photolyses, however, resulted in the retention of the position of the methoxy group, with *exo*-**1** giving the *cis*-diastereomer of the product in a comparatively higher ratio than in solution.[12] A similar selectivity change was also observed for crystalline *endo*-**1**, though with lowered selectivity.

The enhanced selectivity of solid-state photochemical reactions of azoalkanes was also demonstrated by derivative **3**.[11b] While photolysis in solution gave a mixture of the housane **4** and aziridine **5** (with the product ratio depending on the solvent),[13] the photolysis of a crystalline sample gave denitrogenated **4** as the only product, though only in 48% yield. The yield was increased with the irradiation of a powdered sample, which

Department of Chemistry and Biochemistry, University of California, Los Angeles, CA 90095-1569, USA. E-mail: mgg@chem.ucla.edu; Tel: +1 (310) 824 3159

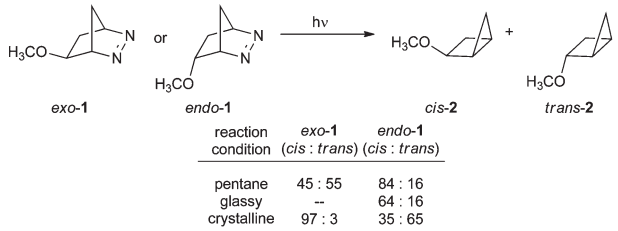

reaction condition	exo-1 (cis : trans)	endo-1 (cis : trans)
pentane	45 : 55	84 : 16
glassy	--	64 : 16
crystalline	97 : 3	35 : 65

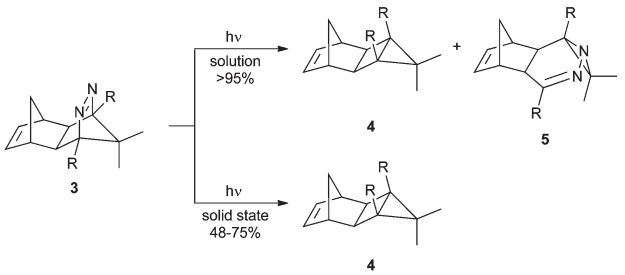

Scheme 2

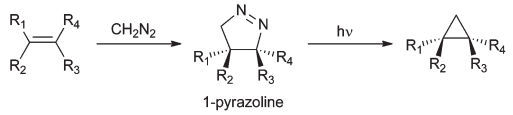

Scheme 3

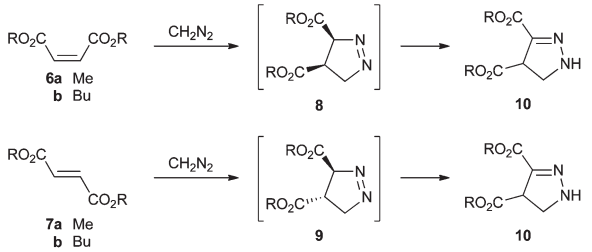

Scheme 4

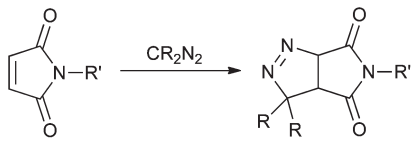

	R'
11a	Me
b	Bu
c	Bn
d	Ph
e	PhPh
f	DMP

	12 R = H yield	13 R = Ph yield
a	98	37
b	100	0
c	99	69
d	100	94
e	100	86
f	100	not clean

Scheme 5

gave a 75% yield with complete selectivity for **4**. The selectivity was attributed to the large rotation of the *gem*-dimethyl groups necessary for the formation of aziridine **5**, which is prevented in the solid state.

While the photochemical decomposition of diazabicyclo [2.2.1]hept-2-enes might be used to explore the generality of the photodenitrogenation reaction in crystalline solids, their synthesis is relatively demanding.[11b,14,15] In contrast, the formation of 1-pyrazolines by the addition of diazoalkanes to activated alkenes is very simple, and thus we decided to use it for this study (Scheme 3).

Preparation and characterization of crystalline pyrazolines

Our initial foray into the synthesis of a set of crystalline pyrazolines was based on the addition of diazomethane to fumarates and maleates substituted with a number of alkoxy groups. We reasoned that a variety of such diesters would allow us to obtain a set of *cis*- and *trans*-, and potentially homochiral, pyrazolines so that we could select those that are crystalline solids for photolysis studies.

Unfortunately, the compounds isolated by addition of diazomethane to dimethyl- and dibutyl maleates **6a,b** and fumarates **7a,b** were shown to isomerize to the corresponding 2-pyrazoline tautomers **10a,b** and thus were not suitable for photolysis studies (Scheme 4).[16] The formation of **10** is in agreement with a previous study by Swieton *et al.*,[17] where it was found that the initially formed 1-pyrazolines tautomerize into the 2-pyrazolines, as determined by ^{1}H NMR and IR spectroscopy. To overcome this issue, we decided to explore the addition of diazomethane to *N*-alkyl maleimides, since the tautomerization of a 1-pyrazoline to give a 2-pyrazoline with a more strained exocyclic double bond is unlikely (Scheme 5).[18] Therefore, maleimides with *N*-methyl (**11a**), *N*-butyl (**11b**), *N*-benzyl (**11c**), *N*-phenyl (**11d**), *N*-4-biphenyl (**11e**) and *N*-3,5-dimethoxyphenyl (DMP, **11f**) groups were prepared and subsequently investigated.

The dipolar cycloaddition reaction of diazomethane with the series of maleimide derivatives **11a–f** in diethyl ether took place in 1 h to yield a white precipitate. The crystalline products were obtained in excellent yields (>98%) and were later identified as pyrazolines **12a–f** (Scheme 5). The ^{1}H NMR spectra of the pyrazoline product showed four doublet of doublet of doublets at *ca.* 3.2, 4.8, 4.9 and 5.7 ppm corresponding to the four hydrogens of the pyrazoline ring.

The addition of diphenyldiazomethane to maleimide derivatives **11a–f** was also studied to obtain products that may be used to determine the effect of substituents on the solution and solid-state photoreactions. The corresponding cycloaddition reactions to form derivatives **13a–f** were much slower relative to the formation of **12a–f** and required overnight stirring. Once again, the products precipitated out as white solids that were nearly insoluble in all solvents, and only sparingly soluble in acetone. Interestingly the ^{1}H NMR spectra of the dissolved diphenyl-substituted products indicated the formation of the denitrogenated cyclopropane. The spectrum of dissolved **13a** matches the literature spectrum of 3-methyl-6,6-diphenyl-3-azabicyclo[3.1.0]-hexane-2,4-dione,[19] instead of that belonging to the pyrazoline.

The sparse solubility of the pyrazoline solids **13** is in stark contrast to the previous report of **13d**, which describes its solubility in chloroform.[20] The reported melting point of 143° also does not agree with our findings, which revealed decomposition for the white precipiate **13d** at *ca.* 151° before melting. However, the only quantitative technique conducted in the

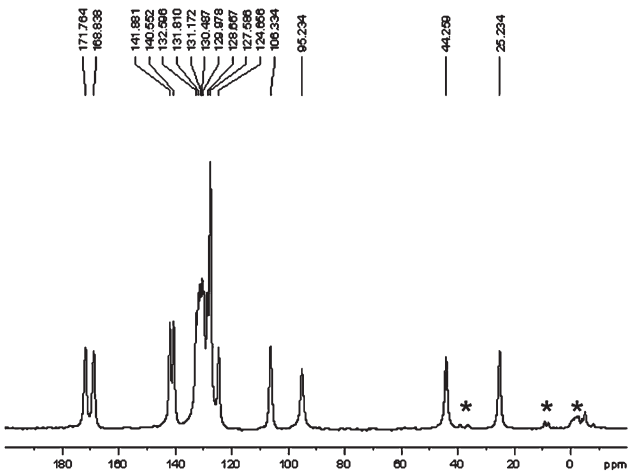

Fig. 1 ^{13}C CP/MAS NMR spectrum of **13a**. Asterisks denote spinning sidebands (MAS = 10 kHz).

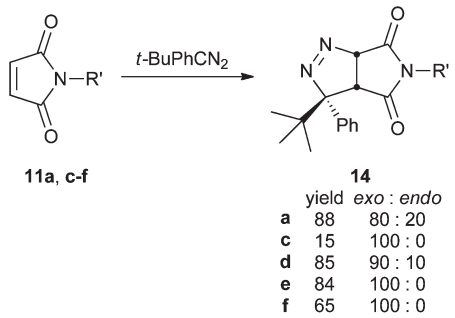

Scheme 6

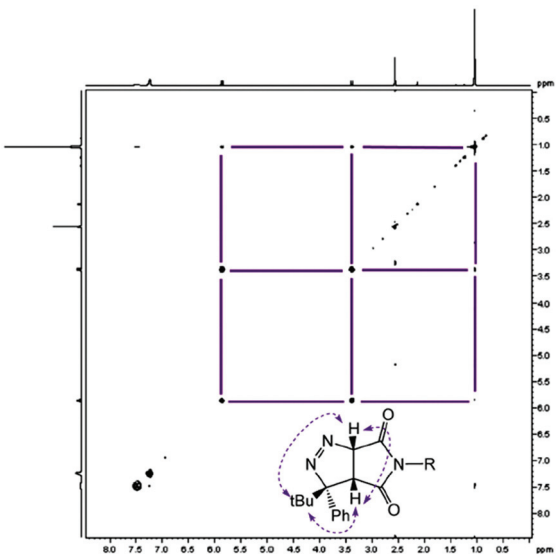

Fig. 2 NOESY spectrum of *exo*-**14a** (R = Me) illustrating through-space correlations that establish the steric relation between the *t*-butyl group and the two pyrazoline hydrogens. They all are on the convex face of the bicyclic system.

previous study was elemental analysis. In our study, solid-state characterization of the white precipitates resulting from the reaction of diphenyldiazomethane with **11a–f** determined that they are in fact the pyrazolines **13**, which subsequently decompose thermally upon dissolution in the NMR solvent. The identity of the precipitated solids as the expected pyrazolines was determined by ^{13}C CP/MAS solid-state NMR analysis. As shown in Fig. 1 with the spectrum of **13a**, the sample contains two non-equivalent carbonyl peaks at 169 and 172 ppm and aliphatic signals at 45, 95 and 106 ppm, which are analogous to the signals for the unsubstituted pyrazolines **12**.[21] The IR spectra of the precipitated solids showed two carbonyl signals in the region of 1701–1718 cm^{-1}, which are also consistent with those determined for the analogous pyrazolines and shifted with respect to those of the starting maleimides (1696–1703 cm^{-1}). The yields for *N*-phenyl and *N*-(4-biphenyl) pyrazolines **13d** and **13e** were good (>86%) while those for *N*-benzyl (**13c**, 69%) and *N*-methyl pyrazolines (**13a**, 37%) were much lower. The addition of diphenyldiazomethane with the more electron rich benzyl (**13b**) and *N*-DMP (**13f**) maleimides either did not take place or gave a mixture of compounds.

In order to also determine whether the photodenitrogenation reaction proceeds diastereoselectively in the solid state, we prepared adducts of the asymmetric *t*-butyl-phenyldiazomethane to maleimides **11a,c–f** to form pyrazolines **14a,c–f** (Scheme 6). *t*-Butyl-phenyldiazomethane was used in hopes that the cycloaddition would be diastereoselective since a *t*-butyl group is much bulkier than a phenyl group. Five equivalents of *t*-butyl-phenyldiazomethane were added to the maleimides and stirred overnight. The product did not precipitate out, as with **12** and **13**, and had to be purified by column chromatography. The ^{1}H NMR spectra showed the characteristic two doublets at *ca.* 3.5 and 6.0 ppm corresponding to the bridgehead protons. The pyrazolines **14a,d–f** formed in moderate to good yields (65–88%).

As predicted, the cycloaddition occurred such that the diastereomer with the *t*-butyl group in the *exo* position was the major diastereomer. The stereochemistry was determined by 2D-NOESY experiments, an example of which is shown for *exo*-**14a** in Fig. 2. The *t*-butyl protons at 1.0 ppm are correlated through space to the nearby bridgehead protons at 3.4 ppm and 5.9 ppm, indicating they are on the same convex side of the bicyclic system. Cycloaddition reactions of *N*-methyl (**14a**) and *N*-phenyl (**14d**) pyrazolines occurred with diastereomeric excesses, de = 60% and de = 80% respectively. However, the minor diastereomer could be isolated only for the methyl pyrazoline (*endo*-**14a**). In the cases of *N*-benzyl (**14c**), *N*-biphenyl (**14e**) and *N*-DMP (**14f**), the *exo*-*t*-butyl pyrazoline formed exclusively. The ^{1}H NMR spectra for these compounds indicate that the *endo*-phenyl substituent does not have the freedom to rotate and the signals for this group at ambient temperature are very broad, as shown in Fig. 3 (top spectrum) for *exo*-**14a**. This assignment was supported by variable temperature ^{1}H NMR analysis, which showed that as the temperature is decreased, the broad signal of the phenyl group (the *endo*-substituent) splits into two peaks that correspond to the non-equivalent halves of the ring (Fig. 3, bottom spectrum).

The melting and thermal stability of the pyrazolines were measured by differential scanning calorimetry (DSC) to determine whether the photochemical reactions were likely to proceed

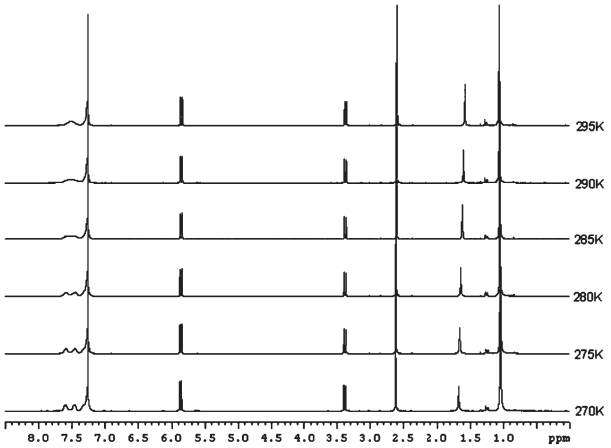

Fig. 3 Variable temperature ^{1}H NMR spectra of *exo*-**14a** illustrating line shape changes in the aromatic region of the spectrum interpreted as a result from hindered rotation of the *endo*-phenyl substituent. (Temperatures are uncorrected.)

Table 1 The melting and decomposition temperatures (°C) of pyrazolines **12**, **13** and **14**

	12 (R = H)		**13** (R = Ph)		**14** (R = *t*-Bu, Ph)[a]	
	Mp	Decomp.	Mp	Decomp.	Mp	Decomp.
a	93	173	—[e]	103	99	152
b	55	154	—[b]	—[b]	—[f]	—[f]
c	101	195	—[e]	130	—[c]	—[c]
d	>180[d]	189	—[e]	151	>157[d]	168
e	—[e]	197	—[e]	146	—[e]	180
f	131	152	—[b]	—[b]	>159[d]	171

[a] Values for *exo*-**14a**. [b] Product not isolated. [c] Not determined due to insufficient sample. [d] Samples decompose before complete melting. [e] Samples decompose before melting. [f] Compound not prepared.

in a solid phase or in mixed solid–liquid two phase systems (Table 1). Based on their melting and decomposition behavior, the pyrazolines can be categorized into three groups. The first class includes those (**12a–c,f**, **14a**) that melt before decomposing, as illustrated by the DCS trace of **12c** in Fig. 4a. While melting occurs at 101 °C, the onset of thermal decomposition is observed at 195 °C. The second class of compounds is represented by **12d**, with a DCS trace shown in Fig. 4b, which begins to melt but decomposition occurs before the phase transition is complete. Finally, the third class is represented in Fig. 4c with pyrazoline **12e**, which decomposes well before its melting point is reached.

From the thermal analysis in Table 1 we conclude that the decomposition temperatures correlate with the 4,4-substituents of the pyrazolines, which should have a direct effect on the stability of the radical center at that position. The unsubstituted pyrazoline **12** has decomposition temperatures that are higher than those of the two substituted pyrazolines **13** and **14**. The diphenyl pyrazolines **13** have the lowest decomposition temperatures, most likely due to the radical stabilizing effects from the two phenyl groups. The diphenyl pyrazolines are unstable at ambient temperature in solution and their thermal reaction occurs in the

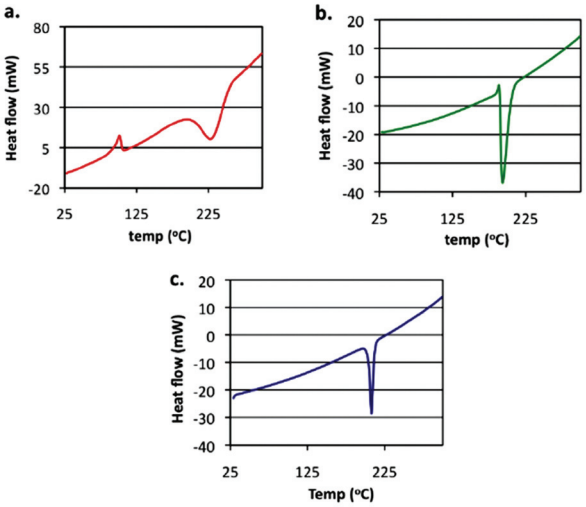

Fig. 4 DSC traces of (a) *N*-benzyl **12c**, (b) *N*-phenyl **12d**, and (c) *N*-(4-biphenyl) **12e**, which illustrate the three different thermal behaviours of the pyrazoline derivatives.

range of *ca.* 100–150 °C in the solid state. Having only one phenyl group that can stabilize the radical center, pyrazolines **14** are stable in solution at ambient temperature and react in the solid state between 150–180 °C.

Photochemical experiments

The denitrogenation of pyrazolines is thought to occur by the stepwise cleavage of the two C–N═N–C bonds to give a 1,3-biradical (Scheme 7). The initial 1,3-biradical[22] formed by photoexcitation may be either a singlet or a triplet, depending on the multiplicity of the excited state reactant. Whether a singlet or a triplet (that eventually intersystem crosses to the singlet state), the 1,3-biradical recombines to give cyclopropane **15** or undergoes two different 1,2 hydrogen shifts to give methyl maleimide **16** or methylene succinimide **17**. It was hoped that the rigid reaction cavity of the solid state would constrain the biradical to undergo recombination and to form only cyclopropane **15**.

Photochemistry of 7-alkyl-2,3,7-triaza-bicyclo[3.3.0]oct-2-ene-6,8-diones 12a–12f in solution and in the solid state. Photochemical experiments in solution were carried out in dilute (2 mg ml^{-1}) solutions of pyrazolines in acetonitrile after removal

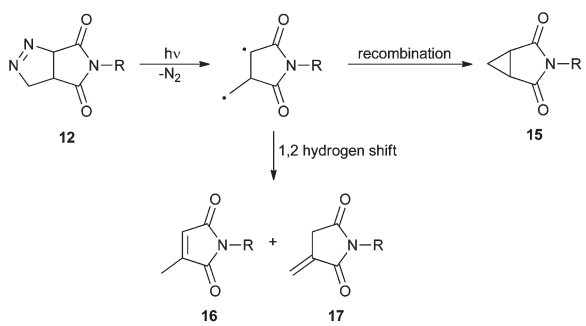

Scheme 7

of oxygen by bubbling argon gas for 10 min. The solutions were exposed to the output of a Hanovia medium pressure mercury vapor lamp through a quartz filter until all the starting material had reacted (*ca.* 2 h). Photochemical reactions in the solid state were carried out with powdered samples spread on a microscope slide until the reaction was completed (24–72 h) or until the solid melted.

Both solution and solid-state reactions were monitored by ^{1}H NMR. The radical recombination product **15** is characterized by a singlet at *ca.* 2.5 ppm, which is assigned to the bridgehead protons that are α to the carbonyl. The 1,2 hydrogen shift product **16** has a doublet at *ca.* 2.2 ppm for the vinylic methyl group and a quartet at *ca.* 6.5 ppm for the vinylic protons, while **17** has apparent triplets at *ca.* 3.3, 5.6 and 6.3 ppm for the succinimide methylene and the two exocyclic methylene hydrogens. Some of the compounds are already known and their assignment was confirmed by comparing their spectra to those available in the literature. This includes compounds **15a**,[23] **15c**,[24] **16a**,[25] **16c**,[26] **16d**,[27] **17a**,[27] **17b**,[28] **17c** and **17d**. For new compounds, the characteristic signals described above were used for identification. As shown in Table 2, while cyclopropenes **15a–15f** were the major products in solution, the selectivity of the reaction varied significantly for different substituents. *N*-Alkyl substituted **12a–12c** gave the corresponding cyclopropenes **15** in yields above 89%. By contrast, the *N*-aryl substituted compounds **12d** and **12e** react with lower selectivities with the hydrogen shift products obtained in higher yields. In all cases, as the reaction progressed, the hydrogen shift products underwent secondary reactions leaving **15** as the only identifiable product. The analysis of compound **12f** was complicated by the overlap of signals from the starting material and signals from product **16f**, but the formation of **17f** in 20% yield is consistent with the results obtained from **12d** and **12e**. Also included in the table are the pyrazoline reactions in the solid state, which proceeded with higher selectivities than those observed in solution. Reactions with powdered samples were carried out until some melting was observed, or until the reaction had gone to completion. Compound **12b**, with a low melting point of 55 °C, could not be reacted at ambient temperature as it immediately started melting. Compound **12a** also started melting at rather low conversion values, despite a melting point of 93 °C, as expected by the fact that the hydrogen shift products are liquids at ambient conditions.[25,27] All the conversion values are indicated in the table except when the extent of conversion was limited by sample melting.

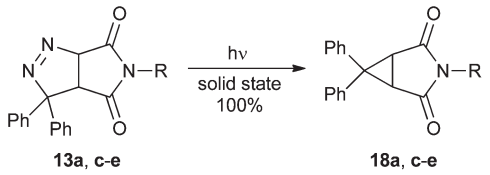

Scheme 8

Photochemistry of 4,4-diphenyl-2,3,7-triaza-bicyclo[3.3.0]oct-2-ene-6,8-diones 13. As indicated in Scheme 8, the solid state photolysis of the 4,4-diphenyl pyrazolines **13a,c–e** gave only the cyclopropane products **18a,c–e**. Solution photolysis could not be investigated for comparison as the pyrazolines were unstable in solution and very rapidly decomposed thermally to the same cyclopropane products. However, the extent of reaction in the solid state could be monitored qualitatively *in situ* by ^{13}C CP/MAS solid-state NMR and ATR-FTIR spectroscopy. While the conversion of **18** was incomplete, the product, which is highly soluble in most organic solvents, could simply be washed off the crystal surface with the unreacted pyrazoline remaining insoluble. The ^{13}C CP/MAS solid-state NMR spectrum of a sample of **13d** after photolysis shows that the reaction takes place upon irradiation in the solid state, and not thermally once dissolved in acetone (Fig. 5). There is a shift in the carbonyl signals from 169.5 and 172.1 ppm in the pyrazoline to 170.3 and 172.6 ppm in the cyclopropane and a more significant shift in the aliphatic signals from 44.8, 95.4 and 106.1 ppm in the pyrazoline to 31.4, 36.7 and 52.4 ppm in the product. While only one carbonyl and two aliphatic signals are expected for the product in solution since the molecule is symmetric, the increased number of signals in the solid-state NMR spectrum suggests that the molecule occupies a general position of symmetry in the crystal lattice, which results in magnetic nonequivalence in an asymmetric environment.

Photochemistry of 4-*exo*-*t*-butyl-4-phenyl-2,3,7-triazabicyclo-[3.3.0]oct-2-ene-6,8-diones 14. Irradiations of *t*-butyl-phenyl analogs *exo*-**14a,d–f** were also explored in acetonitrile and in the solid state. While both hydrogen shift products and two diastereomeric cyclopropanes could have been expected in solution,

Table 2 Product ratios in the photolysis of pyrazolines **12** in solution and in the solid state at 298 K as determined by ^{1}H NMR

		CH_3CN solution		Solid state	
	Mp	Conv.	**15** : **16** : **17**	Conv.	**15** : **16** : **17**
12a	93	100	94 : 0 : 6	17[a]	12 : 0 : 5
12b	55	100	89 : 0 : 11	0[a]	n.a.
12c	101	100	94 : 0 : 6	100	100 : 0 : 0
12d	>180	100	54 : 40 : 6	100	90 : 10 : 0
12e	—	100	47 : 41 : 12	60	48 : 8 : 4
12f	131	96	76 : —[b] : 20	88	82 : —[b] : 6

[a] Sample melted. [b] Signals of **15f** and **16f** are not separable by ^{1}H NMR.

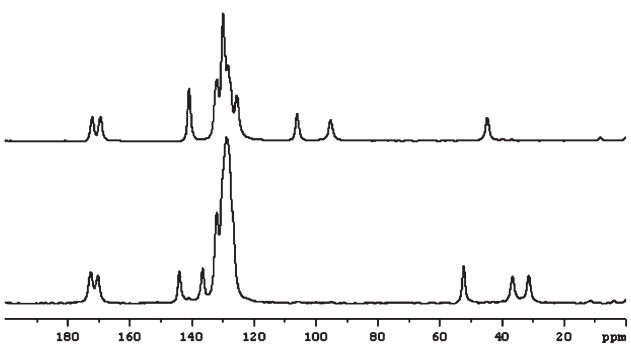

Fig. 5 ^{13}C CP/MAS NMR spectra of pyrazoline **13d** (top) and the solid state photolysis product, cyclopropane **18d** (bottom).

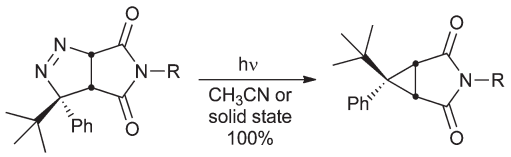

Scheme 9

only one recombination product, *exo*-*t*-butyl cyclopropanes **19a, d–f**, was identified (Scheme 9). The stereochemical identity of the product was verified by a 2D NOESY NMR measurement, which showed the correlation of the *t*-butyl group at *ca.* 1.0 ppm with the bridgehead protons at *ca.* 3.0 ppm (Scheme 9).

Not surprisingly, the solid-state photolysis of pyrazolines *exo*-**14a,d–f** also proceeded very cleanly to give only the cyclopropane product **19a,d–f** in quantitative yields. That only the cyclopropane with retention of stereochemistry is formed, both in solution and in the solid state, indicates that the ring closure of the biradical is faster than bond rotation, which would result in the formation of the other cyclopropane diastereomer. It is also notable that ring closure is faster than the hydrogen shifts.

Conclusions

The addition of diazomethane to fumarates **6** and maleates **7** gave 2-pyrazolines **10** instead of the 1-pyrazolines. This tautomerization was not observed in the products formed by addition of diazomethane to *N*-alkyl maleimides **11a–e**, which gave pyrazolines **12a–f** in nearly quantitative yields (>98%). Analogous reactions carried out with diphenyldiazomethane to form pyrazolines **13a–f** resulted in yields that varied from 0% (*N*-benzyl derivative **13b**) to 94% (*N*-phenyl derivative **13d**) depending on the substituent. The resulting 4,4-diphenyl-pyrazolines were obtained as high-melting crystalline solids insoluble in most organic solvents, which decompose very rapidly into the corresponding cyclopropane upon dissolution in acetone. Therefore, the solid-state reactivity of these crystalline pyrazolines was documented by product characterization using ^{13}C CP/MAS solid-state NMR and FTIR spectroscopy. Finally, the addition of asymmetric *t*-butyl-phenyl-diazomethane takes place diastereoselectively with the larger *t*-butyl group taking the *exo* configuration in *exo*-**14a–e**.

Once the pyrazolines were synthesized, their photolyses were studied in solution and in the solid state. Unsubstituted pyrazolines **12** are low-melting solids and react to give both recombination and 1,2 hydrogen shift products in solution and in the solid state. In agreement with our expectations, reaction selectivities in the solid state were higher than those in solution, although the extent of conversion was limited by some sample melting. The 4,4-diphenyl substituted pyrazolines **13** gave the recombination products in the solid state in quantitative yields but their solution photolyses could not be analyzed at 298 K due to their thermal instability in solution. Finally, the photoinduced denitrogenation of *exo*-**14** also gives recombination products *exo*-**19** both in solution and in the solid state with retention of configuration. Based on these results, we propose that a two step procedure based on the dipolar cycloaddition of diazoalkanes and activated olefins followed by the solid-state denitrogenation of the resulting pyrazolines holds promise for the diastereospecific synthesis of substituted cyclopropanes. Studies currently in progress in our group are aimed at testing this hypothesis.

Materials and methods

N-Alkyl maleimides **12** were prepared according to ref. 29. The spectral data of **12b**,[30a] **12c**[24] and **12d**[31] match the literature spectra.

N-(4-Biphenyl) maleimide 11e

Yellow solid. ^{1}H NMR ($CDCl_3$, 300 MHz): δ 6.87 (2 H, s, 2 × ═CH), 7.35–7.71 (9 H, m, Ph–Ph) ppm. ^{13}C NMR ($CDCl_3$, 75 MHz): δ 126.4, 127.3, 127.8, 128.0, 129.0, 130.5, 134.4, 140.3, 141.1, 169.7 ppm. IR (solid state): ν 3097.4, 1701.2, 1517.8, 1486.0, 1398.1, 1148.5, 835.8, 689.4 cm^{-1}.

N-(3,5-Dimethoxyphenyl) maleimide 11f

Yellow solid. ^{1}H NMR (acetone-d_6, 300 MHz): δ 3.79 (6 H, s, 2 × OCH_3), 6.52 (1 H, t, 2 Hz, Ph), 6.56 (2 H, d, 2 Hz, Ph), 7.00 (2 H, s, 2 × ═CH) ppm. ^{13}C NMR (acetone-d_6, 75 MHz): δ 55.8, 100.2, 105.9, 134.5, 135.2, 161.8, 170.3 ppm. IR (solid state): ν 3095.5, 2967.5, 1708.1, 1600.6, 1476.7, 1207.2, 1149.6, 694.6 cm^{-1}.

General synthesis of diazomethane

Diazomethane was prepared according to ref. 32. Substituted diazomethane was synthesized according to ref. 33 by oxidation of the appropriate hydrazone.

General procedure for the synthesis of 7-alkyl-2,3,7-triazabicyclo[3.3.0]oct-2-ene-6,8-dione 12. Ethereal diazomethane (2 equiv.) was added to *N*-alkyl maleimide **11** dissolved in 10–25 mL ether. The solution was stirred for 1 h. The solvent was evaporated and the product was used without further purification. The spectral data of **12c**[34a] and **d**[34b] match their literature spectra.

7-Methyl-2,3,7-triazabicyclo[3.3.0]oct-2-ene-6,8-dione 12a. White solid. ^{1}H NMR (CD_3CN, 300 MHz): δ 2.79 (3 H, s, NCH_3), 3.23 (1 H, ddd, 10 Hz, 8 Hz, 4 Hz, CHC*H*CH_aH_b), 4.75 (1 H, ddd, 18 Hz, 10 Hz, 2 Hz, CHCHC*H*$_a$H$_b$), 4.86 (1 H, ddd, 18 Hz, 4 Hz, 2 Hz, CHCHCH_a*H*$_b$), 5.69 (1 H, dt, 8 Hz, 2 Hz, C*H*CHCH_aH_b) ppm. ^{13}C NMR (CD_3CN, 75 MHz): δ 25.1, 38.3, 80.7, 95.0, 171.5, 177.4 ppm. IR (solid state): ν 2998.0, 2950.9, 1785.5, 1685.4, 1436.5, 1383.4, 1278.8, 1198.8, 1120.8 cm^{-1}.

7-Butyl-2,3,7-triazabicyclo[3.3.0]oct-2-ene-6,8-dione 12b. White solid. ^{1}H NMR ($CDCl_3$, 300 MHz): δ 0.85 (3 H, t, 7 Hz, C*H*$_3$CH$_2$), 1.20 (2 H, sextet, 7 Hz, CH$_3$C*H*$_2$CH$_2$), 1.44 (2 H, quintet, 7 Hz, CH$_2$C*H*$_2$CH$_2$), 3.23 (1 H, ddd, 10 Hz, 8 Hz, 3 Hz, CHC*H*CH_aH_b), 3.39 (2 H, t, 7 Hz, C*H*$_2$CH$_2$), 4.79 (1 H, ddd, 19 Hz, 10 Hz, 2 Hz, CHCHCH_aH$_b$), 5.02 (1 H, dt, 19 Hz, 3 Hz, CHCHCH_aH_b), 5.69 (1 H, dt, 8 Hz, 2 Hz, C*H*CHCH_aH_b) ppm. ^{13}C NMR ($CDCl_3$, 75 MHz): δ 13.5, 19.9, 29.5, 37.3, 39.0,

80.7, 93.5, 169.6, 175.8 ppm. IR (solid state): ν 2958.6, 1776.7, 1699.1, 1438.2, 1395.2, 1347.1, 1129.3 cm^{-1}.

7-(4-Biphenyl)-2,3,7-triazabicyclo[3.3.0]oct-2-ene-6,8-dione 12e. White solid. ^1H NMR (acetone-d_6, 300 MHz): δ 3.63 (1 H, ddd, 11 Hz, 8 Hz, 4 Hz, CHC*H*CH_aH_b), 4.98 (1 H, ddd, 19 Hz, 11 Hz, 2 Hz, CHCHC*H*$_a$H$_b$), 5.13 (1 H, ddd, 19 Hz, 4 Hz, 3 Hz, CHCHCH_a*H*$_b$), 5.99 (1 H, ddd, 8 Hz, 3 Hz, 2 Hz, C*H*CHCH_aH_b), 7.51–7.78 (9 H, m, Ph–Ph) ppm. ^{13}C NMR (acetone-d_6, 75 MHz): δ 38.8, 81.3, 95.2, 127.9, 128.1, 128.2, 128.6, 129.9, 132.4, 140.9, 142.0, 170.2, 176.4 ppm. IR (solid state): ν 3032.1, 2993.3, 1717.8, 1698.0, 1522.9, 1487.5, 1394.3, 1196.3, 1177.5, 745.9 cm^{-1}.

7-(3,5-Dimethoxyphenyl)-2,3,7-triazabicyclo[3.3.0]oct-2-ene-6,8-dione 12f. White solid. ^1H NMR (CD_3CN, 300 MHz): δ 3.40 (1 H, ddd, 11 Hz, 9 Hz, 3 Hz, CHC*H*CH_aH_b), 3.75 (6 H, s, 2 × OCH_3), 4.85 (1 H, ddd, 19 Hz, 11 Hz, 2 Hz, CHCHCH_aH$_b$), 5.03 (1 H, ddd, 19 Hz, 3 Hz, 3 Hz, CHCHCH_aH_b), 5.81 (1 H, ddd, 8 Hz, 3 Hz, 2 Hz, C*H*CHCH_aH_b), 6.40 (2 H, d, 2 Hz, Ph), 6.55 (1 H, t, 2 Hz, Ph) ppm. ^{13}C NMR (CD_3CN, 75 MHz): δ 38.6, 56.3, 81.3, 95.0, 101.6, 106.4, 134.5, 162.0, 170.4, 176.4 ppm. IR (solid state): ν 3007.6, 2975.0, 1787.9, 1710.2, 1607.8, 1593.7, 1206.9, 1187.2, 1157.6, 1060.1 cm^{-1}.

General procedure for the synthesis of 7-alkyl-4,4-diphenyl-2,3,7-triazabicyclo[3.3.0]oct-2-ene-6,8-dione 13. Ethereal diphenyldiazomethane (5 equiv.) was added to *N*-alkyl maleimide **11** (0.45 mmol) dissolved in 10–25 mL ether and the solution was stirred overnight. To the *N*-methyl and *N*-benzyl reactions, hexane was added and the mixture allowed to stand for 1 h. The white solid was filtered and washed with ether until the diphenyldiazomethane was washed away. The product was used without further purification.

7-Methyl-4,4-diphenyl-2,3,7-triazabicyclo[3.3.0]oct-2-ene-6,8-dione 13a. White solid. ^{13}C CPMAS (MAS 10 MHz): δ 25.2, 44.3, 95.2, 106.3, 124.7, 127.6, 128.7, 130.0, 130.5, 131.2, 131.8, 132.6, 140.6, 141.9, 168.8, 171.8 ppm. IR (solid state): ν 3056.6, 2971.8, 1787.5, 1701.2, 1492.7, 1426.0, 1375.7, 1279.3, 748.9, 697.9 cm^{-1}.

7-Benzyl-4,4-diphenyl-2,3,7-triazabicyclo[3.3.0]oct-2-ene-6,8-dione 13c. White solid. ^{13}C CPMAS (MAS 10 MHz): δ 43.1, 44.6, 97.1, 106.4, 126.0, 128.0, 128.6, 129.7, 131.2, 132.1, 136.5, 140.3, 143.0, 170.5, 174.0 ppm. IR (solid state): ν 3053.5, 3000.1, 1784.2, 1709.4, 1496.3, 1391.9, 1351.4, 1170.7, 742.3, 695.5 cm^{-1}.

4,4,7-Triphenyl-2,3,7-triazabicyclo[3.3.0]oct-2-ene-6,8-dione 13d. White solid. ^{13}C CPMAS (MAS 10 MHz): δ 44.8, 95.4, 106.1, 125.6, 128.4, 130.0, 131.9, 140.9, 169.5, 172.1 ppm. IR (solid state): ν 3057.6, 2962.8, 1718.2, 1595.1, 1494.0, 1379.9, 1179.5, 736.5, 690.0 cm^{-1}.

7-(4-Biphenyl)-4,4-diphenyl-2,3,7-triazabicyclo[3.3.0]oct-2-ene-6,8-dione 13e. White solid. ^{13}C CPMAS (MAS 10 MHz): δ 45.4, 95.0, 105.9, 128.7, 141.2, 142.4, 167.0, 170.5 ppm. IR (solid state): ν 3058.3, 2961.2, 1784.7, 1717.1, 1518.0, 1486.3, 1380.7, 1195.5, 1175.9, 754.5, 697.6 cm^{-1}.

General procedure for the synthesis of 7-alkyl-4-*t*-butyl-4-phenyl-2,3,7-triazabicyclo[3.3.0]oct-2-ene-6,8-dione 14. Ethereal *t*-butyl-phenyl diazomethane (5 equiv.) was added to *N*-alkyl maleimide **11** (0.45 mmol) dissolved in 10–25 mL ether and the solution was stirred overnight. The solution was evaporated. The product was purified by column chromatography (1 : 1 hexane–ether) on silica gel.

4-*endo*-*t*-Butyl-7-methyl-4-phenyl-2,3,7-triazabicyclo[3.3.0]oct-2-ene-6,8-dione *endo*-14a. White solid. ^1H NMR ($CDCl_3$, 300 MHz): δ 1.10 (9 H, s, 3 × CH_3), 3.00 (3 H, s, NCH_3), 3.51 (1 H, d, 9 Hz, C*H*CH), 5.59 (1 H, d, 9 Hz, CHC*H*), 7.28–7.46 (5 H, m, Ph) ppm. ^{13}C NMR ($CDCl_3$, 75 MHz): δ 25.5, 28.4, 38.6, 48.1, 95.0, 109.9, 127.8, 127.9, 127.9, 142.1, 169.0, 174.9 ppm. IR (solid state): ν 3058.6, 2962.8, 1783.6, 1703.4, 1431.0, 1378.5, 1280.4, 1130.6, 705.3 cm^{-1}.

4-*exo*-*t*-Butyl-7-methyl-4-phenyl-2,3,7-triazabicyclo[3.3.0]oct-2-ene-6,8-dione 14a. White solid. ^1H NMR ($CDCl_3$, 300 MHz): δ 1.04 (9 H, s, 3 × CH_3), 2.56 (3 H, s, NCH_3), 3.39 (1 H, d, 8 Hz, C*H*CH), 5.86 (1 H, d, 8 Hz, CHC*H*), 7.24 (3 H, s, Ph), 7.49 (2 H, s, Ph) ppm. ^{13}C NMR ($CDCl_3$, 75 MHz): δ 24.8, 26.3, 39.6, 44.6, 95.3, 108.7, 127.3, 128.0, 136.1, 169.0, 173.5 ppm. IR (solid state): ν 3053.4, 2956.5, 1787.9, 1699.3, 1433.7, 1373.6, 1284.7, 1130.5, 961.6, 708.7 cm^{-1}.

7-Benzyl-4-*exo*-*t*-butyl-4-phenyl-2,3,7-triazabicyclo[3.3.0]oct-2-ene-6,8-dione 14c. White solid. ^1H NMR ($CDCl_3$, 300 MHz): δ 1.05 (9 H, s, 3 × CH_3), 3.38 (1 H, d, 8 Hz, C*H*CH), 4.22 (1 H, d, 14 Hz, CH_aH$_b$), 4.39 (1 H, d, 14 Hz, CH$_a$$H_b$), 5.86 (1 H, d, 8 Hz, CHC*H*), 6.70 (2 H, d, 7 Hz, Ph), 7.03–7.15 (3 H, m, Ph), 7.23 (3 H, s, Ph), 7.49 (2 H, s, Ph) ppm. ^{13}C NMR ($CDCl_3$, 75 MHz): δ 26.3, 39.7, 42.4, 44.5, 95.5, 109.1, 127.5, 127.7, 128.0, 128.0, 128.6, 134.7, 136.2, 168.5, 173.3 ppm.

4-*exo*-*t*-Butyl-4,7-diphenyl-2,3,7-triazabicyclo[3.3.0]oct-2-ene-6,8-dione 14d. White solid. ^1H NMR ($CDCl_3$, 300 MHz): δ 1.45 (9 H, s, 3 × CH_3), 3.50 (1 H, d, 8 Hz, C*H*CH), 6.10 (1 H, d, 8 Hz, CHC*H*), 6.48–6.51 (2 H, m, Ph), 7.22–7.27 (3 H, m, Ph), 7.31 (3 H, s, Ph), 7.52 (2 H, s, Ph) ppm. ^{13}C NMR ($CDCl_3$, 75 MHz): δ 26.5, 39.3, 45.2, 95.0, 109.2, 126.2, 128.1, 128.8, 129.1, 130.9, 136.7, 167.8, 172.9 ppm. IR (solid state): ν 3063.7, 2963.0, 1779.6, 1716.3, 1596.6, 1493.4, 1377.3, 1190.1, 1173.0, 730.4 cm^{-1}.

7-(4-Biphenyl)-4-*exo*-*t*-butyl-4-phenyl-2,3,7-triazabicyclo[3.3.0]-oct-2-ene-6,8-dione 14e. White solid. ^1H NMR ($CDCl_3$, 300 MHz): δ 1.17 (9 H, s, 3 × CH_3), 3.53 (1 H, d, 8 Hz, C*H*CH), 6.13 (1 H, d, 8 Hz, CHC*H*), 6.57 (dd, 7 Hz, 2 Hz, 2H), 7.33–7.57 (12 H, m, Ar) ppm. ^{13}C NMR ($CDCl_3$, 75 MHz): δ 26.7, 39.5, 45.3, 95.0, 109.6, 126.5, 127.3, 127.9, 128.0, 128.3, 128.9, 129.9, 136.7, 140.1, 142.0, 167.8, 173.0 ppm. IR (solid state): ν 3057.3, 2952.2, 1716.0, 1519.0, 1373.6, 1185.0, 759.7 cm^{-1}.

4-*exo*-*t*-Butyl-7-(3,5-dimethoxyphenyl)-4-phenyl-2,3,7-triazabicyclo[3.3.0]oct-2-ene-6,8-dione 14f. White solid. ^1H NMR ($CDCl_3$, 300 MHz): δ 1.15 (9 H, s, 3 × CH_3), 3.48 (1 H, d, 8 Hz, C*H*CH), 3.61 (6 H, s, 2 × OCH_3), 5.58 (2 H, d, 2 Hz, Ph), 6.10 (2 H, d, 8 Hz, CHC*H*), 6.34 (1 H, t, 2 Hz, Ph), 7.30 (4H, s, Ph), 7.58 (1 H, s, Ph) ppm. ^{13}C NMR ($CDCl_3$, 75 MHz): δ 26.6,

39.4, 45.3, 55.6, 94.9, 101.8, 104.5, 109.4, 128.2, 132.3, 136.9, 161.0, 167.5, 172.8 ppm. IR (solid state): ν 3003.7, 2970.0, 1713.5, 1610.8, 1457.7, 1205.9, 1181.5, 1157.1 cm^{-1}.

General procedure for the solution photolysis

The pyrazolines (4–6 mg) were dissolved in 3 mL acetonitrile and the solution was deoxygenated with argon. The solutions were photolyzed with a quartz-filtered medium-pressure Hg Hanovia lamp. The reaction was monitored by ^1H NMR spectroscopy, by taking samples as a function of time throughout the photolysis. Each time a sample was removed, the solution was deoxygenated before the photolysis was continued.

General procedure for the solid-state photolysis

The solid 1-pyrazoline was spread over glass microscope plates and the solid was photolyzed directly with a quartz-filtered medium-pressure Hg Hanovia lamp. The reaction was monitored by ^1H solution NMR or ^{13}C CP/MAS solid-state NMR spectroscopy.

The spectral data of **14a** match literature spectra.[19]

3-Benzyl-6,6-diphenyl-3-azabicyclo[3.1.0]hexane-2,4-dione 18c. ^1H NMR ($CDCl_3$, 300 MHz): δ 3.16 (2 H, s, 2 × CH), 4.07 (2 H, s, CH_2), 6.97–7.35 (15 H, m, 3 × Ph) ppm. ^{13}C NMR ($CDCl_3$, 75 MHz): δ 34.1, 42.0, 50.6, 127.0, 127.5, 127.8, 128.5, 128.6, 128.7, 129.0, 129.2, 129.5, 135.3, 135.7, 141.6, 172.9 ppm. IR (solid state): ν 3064.8, 2952.6, 1762.9, 1689.3, 1493.5, 1438.1, 1400.9, 1340.6, 693.8 cm^{-1}.

3,6,6-Triphenyl-3-azabicyclo[3.1.0]hexane-2,4-dione 18d. ^1H NMR ($CDCl_3$, 300 MHz): δ 3.33 (2 H, s, 2 × CH), 6.33–6.36 (2 H, m, Ph), 7.23–7.57 (13 H, m, Ph) ppm. ^{13}C NMR ($CDCl_3$, 75 MHz): δ 34.0, 50.1, 126.6, 127.1, 128.0, 128.6, 128.7, 129.1, 129.1, 129.6, 129.9, 131.2, 136.3, 141.2, 172.3 ppm. IR (solid state): ν 3063.0, 1770.0, 1703.8, 1598.2, 1495.5, 1375.9, 1174.6, 689.8 cm^{-1}.

3-(4-Biphenyl)-6,6-diphenyl-3-azabicyclo[3.1.0]hexane-2,4-dione 18e. ^1H NMR ($CDCl_3$, 300 MHz): δ 3.53 (2 H, s, 2 × CH), 6.40–6.43 (2 H, m, Ph), 7.28–7.59 (17 H, m, Ar) ppm. ^{13}C NMR ($CDCl_3$, 75 MHz): δ 34.1, 50.2, 126.8, 127.1, 127.3, 127.7, 127.9, 128.1, 128.7, 128.9, 129.2, 129.6, 129.9, 130.3, 136.4, 140.4, 141.2, 141.8, 172.4 ppm. IR (solid state): ν 3058.8, 1774.0, 1707.5, 1598.2, 1494.1, 1387.3, 1182.1, 694.8 cm^{-1}.

6-*exo*-*t*-Butyl-3-methyl-6-phenyl-3-azabicyclo[3.1.0]hexane-2,4-dione 19a. ^1H NMR ($CDCl_3$, 300 MHz): δ 0.90 (9 H, s, 3 × CH_3), 2.14 (3 H, s, NCH_3), 2.83 (2 H, s, 2 × CH), 7.16–7.26 (5 H, m, Ph) ppm. ^{13}C NMR ($CDCl_3$, 75 MHz): δ 23.5, 27.5, 30.3, 34.7, 55.3, 127.9, 127.9, 131.3, 134.7, 174.8 ppm. IR (solid state): ν 3086.0, 2972.2, 1769.0, 1691.7, 1430.4, 1373.3, 994.4, 707.3, 698.6 cm^{-1}.

6-*exo*-*t*-Butyl-3,6-diphenyl-3-azabicyclo[3.1.0]hexane-2,4-dione 19d. ^1H NMR ($CDCl_3$, 300 MHz): δ 0.98 (9 H, s, 3 × CH_3), 3.02 (2 H, s, 2 × CH), 6.20–6.24 (2 H, m, Ph), 7.16–7.19 (3 H, m, Ph), 7.34–7.36 (5 H, m, Ph) ppm. ^{13}C NMR ($CDCl_3$, 75 MHz): δ 27.5, 30.5, 35.0, 54.9, 126.6, 128.2, 128.4, 128.6, 129.0, 131.3, 131.8, 134.8, 173.9 ppm. IR (solid state): ν 3079.1, 2975.2, 1770.5, 1701.7, 1519.6, 1486.9, 1365.1, 1177.4, 763.1, 689.3 cm^{-1}.

3-(4-Biphenyl)-6-*exo*-*t*-butyl-6-phenyl-3-azabicyclo[3.1.0]hexane-2,4-dione 19e. ^1H NMR ($CDCl_3$, 300 MHz): δ 1.00 (9 H, s, 3 × CH_3), 3.05 (2 H, s, 2 × CH), 6.30 (2 H, d, 9 Hz, Ar), 7.29–7.47 (12 H, m, Ar) ppm. ^{13}C NMR ($CDCl_3$, 75 MHz): δ 27.6, 30.6, 35.1, 55.0, 126.8, 127.3, 127.7, 127.9, 128.3, 128.4, 128.9, 130.4, 131.9, 134.8, 140.4, 141.6, 173.9 ppm. IR (solid state): ν 3074.2, 2960.4, 1772.5, 1700.9, 1610.8, 1596.0, 1475.0, 1336.9, 1203.1, 1179.7, 1154.6, 705.3 cm^{-1}.

6-*exo*-*t*-Butyl-3-(3,5-dimethoxyphenyl)-6-phenyl-3-azabicyclo-[3.1.0]hexane-2,4-dione 19f. ^1H NMR ($CDCl_3$, 300 MHz): δ 0.97 (9 H, s, 3 × CH_3), 3.01 (2 H, s, 2 × CH), 3.59 (6 H, s, 2 × OCH_3), 5.32 (2 H, d, 2 Hz, Ph), 6.30 (1 H, t, 2 Hz, Ph), 7.32–7.38 (5 H, m, Ph) ppm. ^{13}C NMR ($CDCl_3$, 75 MHz): δ 27.5, 30.5, 35.0, 54.9, 55.6, 101.8, 104.8, 128.3, 132.0, 132.7, 134.9, 160.9, 173.7 ppm. IR (solid state): ν 3063.9, 2970.6, 1773.3, 1704.9, 1598.8, 1493.4, 1378.4, 1181.6, 697.0 cm^{-1}.

Acknowledgements

We are grateful to the National Science Foundation for support through grants CHE-0844455.

Notes and references

1 (*a*) D. J. C. Constable, C. Jimenez-Gonzalez and R. K. Henderson, Perspective on solvent use in the pharmaceutical industry, *Org. Process Res. Dev.*, 2007, **11**, 133–137; (*b*) R. K. Henderson, C. Jimenez-Gonzalez, D. J. C. Constable, S. R. Alston, G. G. A. Inglis, G. Fisher, J. Sherwood, S. P. Binks and A. D. Curzons, Expanding GSK's solvent selection guide – embedding sustainability into solvent selection starting at medicinal chemistry, *Green Chem.*, 2011, **13**, 854–862.

2 V. H. Grassian, G. Meyer, H. Abruna, G. W. Coates, L. E. Achenie, T. Allison, B. Brunschwig, J. Ferry, M. Garcia-Garibay, J. Gardea-Torresdey, C. P. Grey, J. Hutchison, C. J. Li, C. Liotta, A. Ragauskas, S. Minteer, K. Mueller, J. Roberts, O. Sadik, R. Schmehl, W. Schneider, A. Selloni, P. Stair, J. Stewart, D. Thorn, J. Tyson, B. Voelker, J. M. White and F. Wood-Black, Chemistry for a sustainable future, *Environ. Sci. Technol.*, 2007, **41**, 4840–4846.

3 (*a*) M. A. Garcia-Garibay, The entropic enlightenment of organic photochemistry: strategic modifications of intrinsic decay pathways using an information-based approach, *Photochem. Photobiol. Sci.*, 2010, **9**, 1574–1588; (*b*) M. A. Garcia-Garibay, Advances at the frontiers of photochemical sciences, *J. Am. Chem. Soc.*, 2012, **134**, 8289–8292.

4 (*a*) M. A. Garcia-Garibay, Engineering carbene rearrangements in crystals: from molecular information to solid-state reactivity, *Acc. Chem. Res.*, 2003, **36**, 491–498; (*b*) M. A. Garcia-Garibay, S. Shin and C. N. Sanrame, Engineering reactions in crystalline solids: prediction of intramolecular carbene rearrangements, *Tetrahedron*, 2000, **56**, 6729–6737.

5 C. N. Sanrame, C. P. Suhrada, H. Dang and M. A. Garcia-Garibay, Photochemistry of crystalline chlorodiazirines: the influence of conformational disorder and intermolecular Cl···N═N interactions on the solid-state reactivity of singlet chlorocarbenes, *J. Phys. Chem. A*, 2003, **107**, 3287–3294.

6 (*a*) M. A. Garcia-Garibay and L. Campos, Photochemical decarbonylation of ketones: recent advances and reactions in crystalline solids, in *The Handbook for Organic Photochemistry and Photobiology*, ed. W. Horspool, CRC Press, Boca Raton, FL, 2003, ch. 48; (*b*) C. J. Mortko and M. A. Garcia-Garibay, Engineering stereospecific reactions in crystals: synthesis of compounds with adjacent stereogenic quaternary centers by

photodecarbonylation of crystalline ketones, in *Topics in Stereochemistry*, ed. S. E. Denmark and J. S. Siegel, Wiley-Interscience, Hoboken, NJ, 2006, ch. 7, vol. 25, pp. 205–253.

7 M. J. E. Resendiz, A. Natarajan and M. A. Garcia-Garibay, Diastereoselective synthesis and spin-dependent photodecarbonylation of di(3-phenyl-2-pyrrolidinon-3-yl)ketones: synthesis of nonadjacent and adjacent stereogenic quaternary centers, *Chem. Commun.*, 2008, 193–195.

8 (*a*) A. Natarajan, D. Ng, Z. Yang and M. A. Garcia-Garibay, Parallel syntheses of 8(+)- and 8(−)-α-cuparenone by radical combination in crystalline solids, *Angew. Chem., Int. Ed.*, 2007, **46**, 6485–6487; (*b*) D. Ng, Z. Yang and M. A. Garcia-Garibay, Total synthesis of 8(±)-herbertenolide by stereospecific formation of vicinal quaternary centers in a crystalline ketone, *Org. Lett.*, 2004, **6**, 645–647.

9 For an analogous strategy towards the synthesis of aziridines please see: D. de Loera and M. A. Garcia-Garibay, Efficient aziridine synthesis in metastable crystalline phases by photoinduced denitrogenation of crystalline triazolines, *Org. Lett.*, 2012, **14**, 3874–3877.

10 K. L. Rinehart Jr. and T. V. Van Auken, Light-induced decomposition of pyrazolines. An improved entry into the cyclopropane series, *J. Am. Chem. Soc.*, 1960, **82**, 5251.

11 (*a*) E. L. Allred and R. L. Smith, Thermal and photodecomposition studies with the *exo*- and *endo*-5-methoxy-2,3-diazabicyclo[2.2.1]hept-2-ene system, *J. Am. Chem. Soc.*, 1969, **91**, 6766–6775; (*b*) S. Kohmoto, K. Yamada, U. Joshi, T. Kawatuji, M. Yamamoto and K. Yamada, Photochemical generation of 1,4-diphenybutane-1,4-diyl, *J. Chem. Soc., Chem. Commun.*, 1990, 127–129; (*c*) W. Adam, H. Garcia, V. Marti, J. N. Moorthy, K. Peters and E. M. Peters, Photochemical denitrogenation of norbornene-annelated 2,3-diazabicyclo[2.2.1]hept-2-ene-type azoalkanes: crystal-lattice *versus* zeolite-interior effects, *J. Am. Chem. Soc.*, 2000, **122**, 3536–3537.

12 Although reported as photolyses of crystalline samples of *exo*- and *endo*-**1**, both compounds are oils at room temperature and the crystalline samples were prepared by crystallizing the samples at −80 °C. However, there is limited evidence that these samples are in fact crystalline, and may in fact be supercooled oils.

13 W. Adam, J. N. Moorthy, W. M. Nau and J. C. Scaiano, Solvent effect on product distribution in photochemical pathways of α C–N *versus* β C–C cleavage of n,π* triplet-excited azoalkanes, *J. Am. Chem. Soc.*, 1997, **119**, 5550–5555.

14 P. D. Bartlett and N. A. Porter, The stereochemical course of cyclic azo decompositions, *J. Am. Chem. Soc.*, 1968, **90**, 5317–5318.

15 (*a*) G. E. Collis and D. Wege, Approaches to cyclopropa-fused quinones. The synthesis and photolysis of some 4,9-disubstituted 3,3-dimethyl-*3H*-benz[*f*]indazoles, *Aust. J. Chem.*, 2003, **56**, 903–908; (*b*) C. Alcaraz, M. D. Fernandez, M. Pilar de Frutos, J. L. Marco, M. Bernabe, C. Foces-Foces and F. H. Cano, Asymmetric syntheses of 1-amino-2-phenyl-(alkyl)-cyclopropanecarboxylic acids by diastereoselective cyclopropanation of highly functionalized monochiral olefines, *Tetrahedron*, 1994, **50**, 12443–12456; (*c*) W. Adam, C. P. Librera, F. G. Klarner and F. Wurche, Stereochemical memory in the regioselective and diastereoselective rearrangement of tricyclo[3.3.0.$0^{2,4}$]octanes (housanes) by electron transfer (1,3-cyclopentanediyl radical cations) and acid (cyclopentyl carbenium ions) and silver-ion catalysis, *J. Am. Chem. Soc.*, 2003, **125**, 995–1001; (*d*) T. Wakamiya, Y. Oda, H. Fujita and T. Shiba, Synthesis and stereochemistry of carnosadine, a new cyclopropyl aminio acid from red alga *Grateloupia carnosa*, *Tetrahedron Lett.*, 1986, **27**, 2143–2144; (*e*) P. A. Wender, J. M. Kee and J. M. Warrington, Practical synthesis of prostratin, DPP and their analogs, adjuvant leads against latent HIV, *Science*, 2008, **320**, 649–652; (*f*) M. Oba, N. Nishiyama and K. Nishiyama, Synthesis and reactions of a novel 3,4-didehydropyroglutamate derivative, *Chem. Commun.*, 2003, 776–777.

16 The IR spectra of **10** are characterized by the N–H stretch at *ca.* 3360 cm^{-1} and C=O stretches at 1730 and 1700 cm^{-1}.

17 G. Swieton, J. von Jouanne, H. Kelm and R. Huisgen, Effect of pressure on the 1,3-dipolar cycloaddition reaction of diphenyl-diazomethane to carbon–carbon multiple bonds, *J. Org. Chem.*, 1983, **48**, 1035–1040.

18 R. B. Turner and R. H. Garner, Heats of hydrogenation. V. Relative stabilities in certain exocyclic-endocyclic olefin pairs, *J. Am. Chem. Soc.*, 1958, **80**, 1424–1430.

19 H. E. Zimmerman and O. D. Mitkin, The aza-type-B photochemical rearrangement: the role of a second carbonyl in heterocyclic photochemistry. Mechanistic and exploratory organic photo-chemistry, *J. Org. Chem.*, 2007, **72**, 6091–6096.

20 A. Mustafa, S. M. A. D. Zayed and S. Khattab, Reactions with diazoalkanes. V. Action of diazoalkanes and of aryl azides on *N*-arylmaleimides, *J. Am. Chem. Soc.*, 1956, **78**, 145–149.

21 The ^{13}C CP/MAS spectra were acquired at a ^{13}C frequency of 75 MHz and a ^{1}H frequency of 300 MHz using a ^{1}H ninety degree ($\pi/2$) pulse width of 4.00 μs, a Hartmann–Hahn contact time of 5 ms, a data acquisition time of 66 ms, and a recycle delay of greater than five times the spin-lattice relaxation time of the protons. The sample was spun at a MAS rate of 10 MHz.

22 M. Abe, J. Ye and M. Mishima, The chemistry of localized singlet 1,3-diradicals (biradicals): from putative intermediates to persistent species and unusual molecules with a π-single bonded character, *Chem. Soc. Rev.*, 2012, **41**, 3808–3820.

23 C. D. Poulter and R. B. Dickson, Stereospecific $^{5}J_{H-H}{}^{6}J_{H-H}$ couplings in 3-methyl-3-azabicyclo[3.1.0]hexan-2,4-dione, *Tetrahedron Lett.*, 1971, **12**, 2255–2258.

24 M. Ostendorf, R. Romagnoli, I. C. Pereiro, E. C. Roos, M. J. Moolenaar, W. N. Speckamp and H. Hiemstra, Oxazaborolidine catalysed enantioselective reduction of cyclic *meso*-imides, *Tetrahedron: Asymmetry*, 1997, **8**, 1773–1789.

25 G. B. Gill, G. D. James, K. V. Oates and G. Pattenden, The synthesis of 5-ylidenepyrrol-2-(5*H*)-ones from maleimides and from pyrrol-2-(5*H*)-ones, *J. Chem. Soc., Perkin Trans. 1*, 1993, 2567–2579.

26 M. Yogo, K. Hirota and Y. Maki, Synthesis of 5-iminopyrrol-2-one derivatives from 1,3-oxazines. Ring transformations *via* attack on the 2- or 6-position of 1,3-oxazines, *J. Chem. Soc., Perkin Trans. 1*, 1984, 2097–2102.

27 O. Tsuge, S. Kanemasa, S. Kuraoka and S. Takenaka, New C–C bond formation with pyridinium methylide: hydromethylenation of olefins, *Chem. Lett.*, 1984, **13**, 281–284.

28 T. Oishi, M. Momoi, M. Fujimoto and T. Kimura, Reactivities of *N*-alkylitaconimides in radical copolymerizations with styrene or methyl methacrylate, *J. Polym. Sci., Part A: Polym. Chem.*, 1983, **21**, 1053–1063.

29 T. F. Braish and D. E. Fox, A practical synthesis of *N*-substituted maleimides, *Synlett*, 1992, 979–980.

30 (*a*) B. Pal, P. K. Pradhan, P. Jaisankar and V. S. Giri, First triphenyl-phosphine-promoted reduction of maleimides to succinimides, *Synthesis*, 2003, 1549–1552; (*b*) P. Garner, W. B. Ho, S. K. Grandhee, W. J. Youngs and V. O. Kennedy, Development of an asymmetric approach to the 3,8-diazabicyclo[3.2.1]octane moiety of quinocarcin *via* intramolecular 1,3-dipolar cycloadditions of photochemically generated azomethine ylides, *J. Org. Chem.*, 1991, **56**, 5893–5903.

31 W. I. Awad, S. M. Abdel, R. Omran and M. Sobhy, Notes-reactions with diazoalkanes. I. Action of diazomethane on *N*-phenylmaleimide, with a special note on the pyrolysis products of the pyrazoline, *J. Org. Chem.*, 1961, **26**, 4126–4128.

32 C. J. Mortko, *PhD dissertation*, University of California, Los Angeles, 2005.

33 *US Pat.*, 5 587 464, 1996.

34 (*a*) S. Kim, W. Won and Y. Kang, Ring opening reaction of pyrazolo[3,4-*c*]-maleimide nucleosides, *Nucleosides Nucleotides*, 1997, **16**, 2025–2033; (*b*) M. W. Majchrzak and A. Kotelko, Thermolysis of 7-phenyl-2,3,7-triazabicyclo[3.3.0]oct-2-ene-6,8-dione, *J. Heterocycl. Chem.*, 1985, **22**, 1475–1477.